Electrostatic interactions between the CTX phage minor coat protein and the bacterial host receptor TolA drive the pathogenic conversion of *Vibrio cholerae*

Received for publication, March 13, 2017, and in revised form, June 21, 2017 Published, Papers in Press, June 22, 2017, DOI 10.1074/jbc.M117.786061

Laetitia Houot[1], **Romain Navarro**[2], **Matthieu Nouailler**, **Denis Duché**, **Françoise Guerlesquin**, and **Roland Lloubes**

From the Laboratoire d'Ingénierie des Systèmes Macromoléculaires, UMR7255, Institut de Microbiologie de la Méditerranée, Aix-Marseille Université–CNRS, 31 Chemin Joseph Aiguier, 13402 Marseille Cedex 20, France

Edited by Chris Whitfield

Vibrio cholerae **is a natural inhabitant of aquatic environments and converts to a pathogen upon infection by a filamentous phage, CTXΦ, that transmits the cholera toxin-encoding genes. This toxigenic conversion of *V. cholerae* has evident implication in both genome plasticity and epidemic risk, but the early stages of the infection have not been thoroughly studied. CTXΦ transit across the bacterial periplasm requires binding between the minor coat protein named pIII and a bacterial inner-membrane receptor, TolA, which is part of the conserved Tol-Pal molecular motor. To gain insight into the TolA–pIII complex, we developed a bacterial two-hybrid approach, named Oxi-BTH, suited for studying the interactions between disulfide bond-folded proteins in the bacterial cytoplasm of an *Escherichia coli* reporter strain. We found that two of the four disulfide bonds of pIII are required for its interaction with TolA. By combining Oxi-BTH assays, NMR, and genetic studies, we also demonstrate that two intermolecular salt bridges between TolA and pIII provide the driving forces of the complex interaction. Moreover, we show that TolA residue Arg-325 involved in one of the two salt bridges is critical for proper functioning of the Tol-Pal system. Our results imply that to prevent host evasion, CTXΦ uses an infection strategy that targets a highly conserved protein of Gram-negative bacteria essential for the fitness of *V. cholerae* in its natural environment.**

Phage/bacterium interaction is one of the driven forces for gene acquisition and bacterial host adaptation to their environment, and it has been frequently associated with increased virulence of the bacterial host. A striking example of this parasitism-dependent adaptation is *Vibrio cholerae*, a bacterial natural inhabitant of estuaries, and the causative agent of epidemic disease cholera. Although there are more than 200 O-antigen serogroups described, only two have been reported to cause the pandemic disease cholera, the O1 and O139 serotypes, due to the production of two essential virulence factors, the toxin co-regulated pilus (TCP)[3] and the cholera toxin (CT). Interestingly, the genes *ctxAB* encoding the enterotoxin CT are not carried by the core genome of the bacterium but can be acquired after infection by a lysogenic bacteriophage known as CTXΦ (1). Once infected, the bacterium produces CT and assembles new phage particles (carrying the *ctxAB* genes) that will be secreted in the environment, and it may convert non-pathogenic *V. cholerae* cells to pathogenicity.

Most of the knowledge on CTXΦ infection have been extrapolated from the canonical model of *Escherichia coli* F-pilus-specific coliphages Ff (including f1Φ, fdΦ, and M13Φ). CTXΦ and FfΦ both belong to the genus *Inovirus,* which are filamentous particles containing a circular single-stranded DNA genome. The genome of inoviruses includes about 10 genes and is generally organized in a conserved modular structure in which functionally related genes are grouped together (2, 3). FfΦ and CTXΦ binding and uptake into the host cell rely primarily on the minor coat protein pIII located at the distal tip of the phage and present at three to five copies. Although there is no sequence conservation between $pIII^{Ff}$ and $pIII^{CTX}$, both proteins are composed of three distinct domains separated by two low-complexity regions that serve as linkers. Although the N-terminal (N1) and the central domains (N2) are exposed at the capsid surface, the C-terminal domain (N3) anchors the pIII protein to the phage particle through hydrophobic interactions (4–6).

Filamentous phage infection of the bacterial host is seen as a sequential two-step process. First, phage recruitment occurs upon specific binding between the phage capsid pIII-N2 domain and a primary receptor exposed at the surface of the cell host, the conjugative F pilus for *E. coli* (3, 7) and the TCP for *V. cholerae* (1, 5). In *E. coli*, ATP-dependent retraction of the F pilus brings the phage in contact with the cell envelope, promoting its transport across the outer membrane (OM) by an unknown mechanism. Then, pIII must partially unfold to separate N1 and N2 domains (8). This event is crucial in the infec-

This work was supported in part by CNRS and the Aix-Marseille Université (to the R. L. and W. G. Laboratories) and Agence Nationale de la Recherche Grant ANR-14-CE09-0023 (to the R. L. research team). The authors declare that they have no conflicts of interest with the contents of this article.
This article contains supplemental Figs. S1–S6 and Tables S1–S2.
[1] Supported by Postdoctoral Fellowship FRM, SPF20100518724 from Fondation pour la Recherche Medicale. To whom correspondence should be addressed. Tel.: 33-491-164-663; Fax: 33-491-712-124; E-mail: E-mail: lhouot@imm.cnrs.fr.
[2] Supported by a Ph.D. fellowship from the French Ministry of Research.

[3] The abbreviations used are: TCP, toxin co-regulated pilus; IPTG, isopropyl 1-thio-β-D-galactopyranoside; CT, cholera toxin; PDB, Protein Data Bank; OM, outer membrane; IM, inner membrane; BACTH, bacterial two-hybrid; DOC, deoxycholate; HSQC, heteronuclear single quantum coherence; Sm, streptomycin; Cm, chloramphenicol.

tion process as it unmasks the pIII-N1 domain for subsequent binding to a second receptor, the TolA^{Ec} protein located in the cell envelope (8–12). In *E. coli*, it has been proposed that the pIII-N1^{Ff}/TolAIII^{Ec} interaction triggers conformational modifications permitting the pIII-N3 domain to form a pore in the bacterial IM, allowing the subsequent phage DNA injection into the cell cytoplasm (13). The nature of the force driving the DNA out of the capsid remains unknown.

In *V. cholerae,* TCP retraction seems central to the phage infection process, as TCP production alone is not sufficient to allow CTXΦ uptake (14). Although TCP parasitism facilitates the introduction of CTXΦ into the host cell, subsequent phage binding to TolA^{Vc} appears to be the limiting step of the infection process (5, 6, 15). Thus, Heilpern and Waldor (5) have shown that a chimeric fd phage displaying the pIII-N1^{CTX} domain fused to the pIII-N3^{fd} domain can successfully infect *V. cholerae* cells. This demonstrates that the pIII-N1^{CTX} domain displayed at the tip of the capsid is critical and sufficient to ensure host-specific recognition in a TCP-independent manner (5).

TolA is the central protein of the Tol-Pal cell envelope system, which is highly conserved in Gram-negative bacteria (16, 17). In addition to TolA, the Tol-Pal complex is composed of two IM proteins, TolQ and TolR, of the OM lipoprotein Pal and of the periplasmic protein TolB. In several species, including *E. coli* and *V. cholerae*, two additional proteins complete the system, the periplasmic protein CpoB (previously YbgF) (18) and the cytoplasmic thioesterase YbgC (19). The Tol-Pal complex is suspected to function as a nanomachine, using the proton-motive force of the IM to generate movements and to transfer energy to OM proteins. Multiple interactions connecting the different components of the Tol-Pal system have been identified. TolA, TolQ, and TolR form a complex anchored in the IM. The TolA protein extends in the periplasm thanks to a long α2-helix (TolAII domain), whereas its globular C-terminal domain (TolAIII) interacts with TolB, and with Pal in the presence of proton-motive force (20–22). Moreover, Pal interacts with TolB and with the peptidoglycan (23). Thus, the Tol-Pal system links the IM, the OM, and the peptidoglycan. The system is involved in maintaining OM integrity, conferring pleiotropic phenotypes when one of its genes is mutated: increased sensitivity to detergents, cell filamentation in low and high osmolarity media, and outer membrane hypervesiculation (6, 16). In addition, the Tol system is involved in the late stage of cell division corresponding to the OM constriction (25) and has been found associated with the PBP1B–LpoB complex in *E. coli* (18). It is also required for proper localization of polar factor in *Caulobacter crescentus* (26) and of chemoreceptors in *E. coli* (27).

For both coliphage and CTXΦ, structural studies on isolated protein domains have provided new insights into the complex formed with TolAIII in the bacterial periplasm (Fig. 1). First, the structures demonstrate that although the CTXΦ pIII-N1 and M13Φ pIII-N1 domains have only 15% sequence identity, they are both dominantly composed of β-strands, and multiple disulfide bonds stabilize their structures. On the bacterial side, TolAIII^{Ec} and TolAIII^{Vc} are curved structures mixing α-helices and β-sheets. A high-resolution structure of *E. coli* TolAIII free in solution has been obtained by heteronuclear NMR (Protein Data Bank PDB code 1S62) (12), whereas the TolAIII in complex with coliphage pIII-N1^{M13} (residues 11–86) has been obtained by X-ray crystallography (PDB code 1Tol). The structure shows that the pIII-N1^{M13} domain binds the concave side of TolAIII^{Ec}, forming a continuous interprotein β-sheet (8). In 2012, Ford *et al.* (15) determined the crystal structure of pIII-N1^{CTX} domain alone and in complex with the *V. cholerae* TolAIII domain (PDB code 4G7X). Surprisingly, the authors showed that pIII-N1^{CTX} binds on the convex face of TolAIII^{Vc}, resulting in a continuous interprotein β-sheet (Fig. 1*A*). Thus, interaction between the two partners delineates a distinct interface compared with the coliphage model of infection (15).

Filamentous phages are not the only particles that parasitize the Tol-Pal system to penetrate *E. coli* cells. Colicins are bacterial toxins comprising various types of lethal activity targeting the IM, the RNA, or the peptidoglycan of its bacterial target. Tol-dependent colicins have been shown to interact with one or more of the Tol proteins during their translocation across the periplasm, showing some similarities with Tol-dependent filamentous phage uptake. In 2012, Li *et al.* (28) demonstrated that a colicin A peptide (residues 53–107) binds on the convex face of TolAIII^{Ec}, forming an intermolecular antiparallel β-sheet.

It is puzzling to observe that despite the structural similarities between *V. cholerae* and *E. coli* TolAIII domains, the molecular binding interfaces with colicin A, pIII^{CTX}, and pIII^{M13} differ, illustrating the versatile functioning of TolA as a periplasmic hub protein. In this study, our goal was to investigate the determinants allowing CTXΦ-specific host selection and periplasm transit *in vivo* thanks to a new oxidative bacterial two-hybrid approach combined to NMR and *in vivo* studies.

Results

Development of an oxidative bacterial two-hybrid approach dedicated to disulfide bond-folded protein analysis

To gain insights into the mechanism of CTXΦ transit through the periplasm, we first analyzed the interaction that occurs between pIII-N1^{CTX} and TolAIII^{Vc}, compared with the pIII-N1^{M13} and TolAIII^{Ec} interaction, using a bacterial two-hybrid (BACTH) approach. This system relies on the reconstitution of the signaling cAMP transduction cascade in an endogenous adenylate cyclase-deficient strain (29). The TolAIII domains from *V. cholerae* and from *E. coli* were fused to the T18 domain in the pUT18 vector, whereas the pIII-N1 domains from M13 and CTX phages were fused to the T25 domain in the pKT25 vector. Constructs were introduced into the *E. coli* BTH101 strain, and co-transformants were tested on MacConkey plates. As a control, we first observed that in this assay, the T18-TolAIII^{Ec} construct gives a positive interaction signal with the colicin A N-terminal domain (ColA^{N}) as described previously (10, 22, 30), which validated our approach (Fig. 1*B*, *left panel*). We also observed that a T18-TolAIII^{Vc} construct is unable to bind T25-ColA^{N}, attesting the specificity for partner recognition between the two bacterial species. Then, we tested

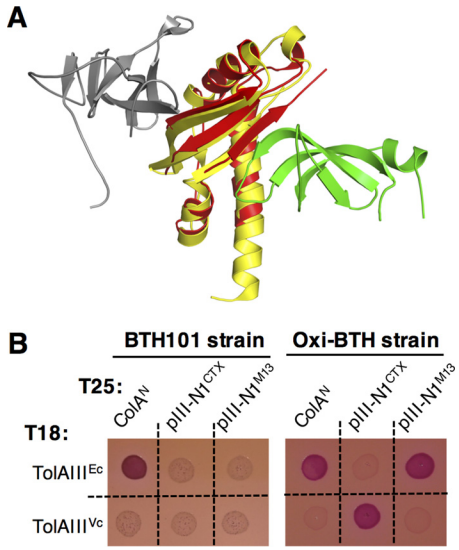

Figure 1. pIII-N1^{CTX} and pIII-N1^{M13} domains specifically interact with their cognate TolA partner. *A,* crystal structure of *V. cholerae* TolAIII (*yellow*) in complex with CTXΦ pIII-N1 (*gray,* PDB code 4G7X, and superimposed to *E. coli* TolAIII (*red*) in complex with M13Φ pIII-N1 (*green,* PDB code 1TOL). *B,* bacterial two-hybrid assay: *E. coli* BTH101 or Oxi-BTH reporter cells producing the indicated domains fused to the T18 or T25 domain of the *Bordetella pertussis* adenylate cyclase were spotted on MacConkey plates. The *red* color of the spot reflects the interaction between tested domains. ColA^{N} (N-terminal colicin A domain), pIII-N1^{CTX} (N-terminal domain of CTXΦ pIII protein), pIII-N1^{M13} (N-terminal domain of M13-phage pIII protein), and TolAIII (C-terminal domain of *E. coli* or *V. cholerae* TolA protein).

the TolAIII^{Vc} and pIII-N1^{CTX} constructs together, but we did not detect interaction between these different domains. We obtained the same negative result when we tried to detect the TolAIII^{Ec}/pIII-N1^{M13} interaction (Fig. 1*B*, *left panel*). We hypothesized that this result could arise from improper folding of disulfide-bonded TolAIII, pIII-N1^{M13}, or pIII-N1^{CTX} domains when expressed in the cell cytoplasm (Fig. 2, *A* and *B*).

Thus, we envisioned that a bacterial two-hybrid assay in an oxidative environment would allow the proper folding of proteins with disulfide bonds. Several *E. coli* strains, such as Origami (Novagen) or SHuffle (New England Biolabs), have been engineered to optimize the purification of proteins with disulfide bonds and are commercially available. We chose the SHuffle T7 strain as a chassis because it is deleted for glutaredoxin reductase (*gor*) and thioredoxin reductase (*trxB*) genes, allowing disulfide bond formation in the cytoplasm. In addition, this strain expresses a cytoplasmic version of the disulfide bond isomerase DsbC, promoting correct disulfide bond formation and proper oxidative folding of proteins containing multiple cysteines (31). We transduced the *cya* mutation in the SHuffle strain to make the Oxi-BTH strain (for Oxidative Bacterial Two-Hybrid). The resulting strain was co-transformed with the pUT18 and pKT25 vectors expressing domains of interest. As shown in Fig. 1*B* (*right panel*), the Oxi-BTH strain allowed the detection of interaction between TolAIII^{Vc} and pIII-N1^{CTX}, as well as between TolAIII^{Ec} and pIII-N1^{M13}. Thus, we concluded that the Oxi-BTH strain is a powerful tool to apply the BACTH system to the study of disulfide-bonded proteins. Indeed, our data suggest that in both *E. coli* and *V. cholerae*, disulfide bond-dependent folding of the TolAIII domain and/or the phage minor capsid domain is required to allow binding of the two partners. Conversely, TolAIII ^{Ec} is able to interact with the colicin A N-terminal domain, which does not contain cysteines, in both reducing and oxidizing conditions (Fig. 1*B*). Finally, we did not observe cross-interaction between the two species (*i.e.* TolAIII^{Vc}/pIII-N1^{M13} or TolAIII^{Ec}/pIII-N1^{CTX}) despite strong structural conservation between *E. coli* and *V. cholerae* TolAIII domains.

Role of disulfide bonds in TolAIII^{Vc}/pIII-N1^{CTX} interaction

Because the TolAIII^{Vc}/pIII-N1^{CTX} interaction is only seen in our oxidative two-hybrid assay, we hypothesized that one or more disulfide bonds might be essential for bacterial and phage domain recognition. To test this hypothesis, each disulfide bond (one in TolAIII^{Vc} and four in pIII-N1^{CTX}, Fig. 2, *A* and *B*) was sequentially abolished by introducing substitutions of individual cysteine to serine in the BACTH constructs. The resulting mutants were then tested in the Oxi-BTH assay. As shown in Fig. 2*C*, TolAIII^{Vc} (C292S) construct was still able to interact with pIII-N1^{CTX}. This suggests that disulfide bond formation in TolAIII^{Vc} is not required for CTX phage binding. We then targeted each of the four disulfide bonds present in pIII-N1^{CTX}. None of the individual mutations we performed was able to totally abolish binding to TolAIII^{Vc}. Interestingly, mutation of the second or the third S–S bond (mutations C47S and C75S, respectively) of the phage pIII-N1 domain resulted in a faint interaction signal, suggesting a weaker binding affinity between TolAIII^{Vc} and these two pIII-N1^{CTX} mutants compared with the wild-type construct. In agreement with this observation, a pIII-N1^{CTX}(C47S/C75S) double mutant was not able to interact with TolAIII^{Vc}. These observations are unlikely to result from stability defects of the cysteine variants compared with the native pIII-N1 protein. Indeed, inserting the same mutations on the His-tagged pIII-N1^{CTX} domain expressed from the pIN vector resulted in equivalent expression of the different constructs (supplemental Fig. S1). Moreover, as the pIII-N1^{CTX}/TolAIII interaction is not seen in the regular BACTH assay, it is more likely that pIII-N1^{CTX} folding via its 2nd and 3rd disulfide bonds is critical for TolAIII^{Vc} binding.

CTXΦ central domain pIII-N2 does not block phage pIII-N1 accessibility to TolAIII^{Vc}

It has been shown that Ff coliphages require an activation step to become able to infect the host cell. Indeed, in the native conformation of the minor capsid protein pIII^{Ff}, the N2 domain is tightly associated with N1, which buries the phage TolAIII-binding site at the domain interface. Phage activation is processed upon binding of N2 to the primary receptor, the F pilus, which initiates partial unfolding, prolyl cis-to-trans isomerization in the hinge between N1 and N2 and domain disassembly, thereby exposing its binding site for the ultimate receptor TolA (32). It has been proposed that the isomerization sets a molecular timer to maintain the binding-active state long enough for the phage to interact with TolA. Conversely, Craig and coworkers (15) have suggested that the TolA-binding site on pIII-

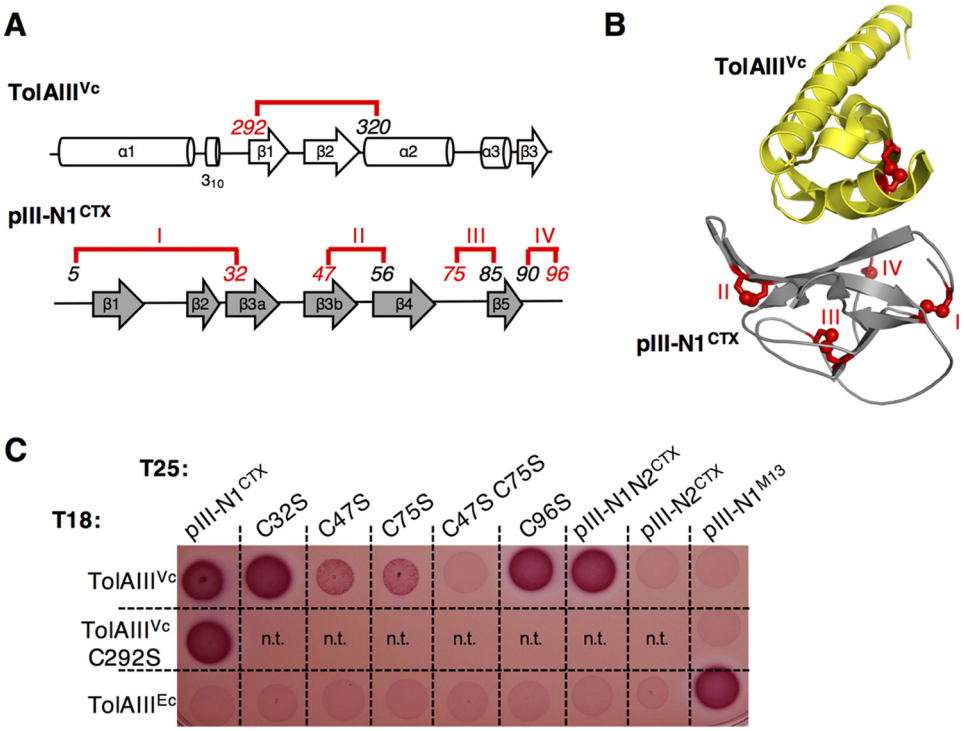

Figure 2. pIII-N1^{CTX} disulfide bonds II and III are required for TolAIII^{Vc} interaction. *A,* schematic representation of disulfide bond localization (15) on the secondary structure of TolAIII^{Vc} and pIII-N1^{CTX}; *B,* representation of disulfide bonds on the crystal structure of the complex. Disulfide bonds in pIII-N1 are numbered *I–IV* and colored in *red. Italic numbers* refer to cysteine residue positions. *C,* oxidative bacterial two-hybrid assay: Oxi-BTH reporter cells producing the T25 domain fused to pIII-N1^{CTX}, pIII-N1N2^{CTX}, or pIII-N2^{CTX} domains and the T18 domain fused to *V. cholerae* TolAIII were spotted on MacConkey plates. Variants bearing substitutions aimed to abolish each of the four disulfide bonds in the pIII-N1^{CTX} domain (C32S, C47S, C75S, and C96S) or in TolAIII^{Vc} (C292S) are presented. TolAIII^{Ec} and pIII-N1^{M13} are used as a controls. *n.t.,* not tested.

N1^{CTX} is permanently accessible and does not require initial pilus-induced conformational change. We wondered whether a fusion to the two-hybrid T25 domain would allow us to test the influence of pIII-N2^{CTX} on the accessibility of pIII-N1^{CTX} in an Oxi-BTH interaction assay. Indeed, our data show that the T25–pIII-N1N2^{CTX} construct is able to bind T18–TolAIII^{Vc}, whereas the T25–pIII-N2^{CTX} domain alone is not (Fig. 2*C*). This result demonstrates that pIII-N1^{CTX} exposes a TolAIII^{Vc}-binding motif that is not masked by the pIII-N2 domain.

Specific recognition between the TolAIII^{Vc} and pIII-N1^{CTX} domains relies on two salt bridges

We aimed to identify the residues showing a predominant role in the specificity of binding. Reversible protein/protein interactions involve low energy ionic bonds, hydrogen bonds, and van der Waals interactions. Based on the co-crystal structure of TolAIII^{Vc} and pIII-N1^{CTX} (PDB code 4G7X (15)), we focused our analysis on the intermolecular salt bridges. Residues Lys-324, Arg-325, and Lys-347 on TolAIII^{Vc}, respectively, interact with Glu-37, Asp-39, and Glu-92 on pIII-N1^{CTX} (Fig. 3*A*). To analyze the importance of these three salt bridges in the complex formation, we abolished them sequentially by introducing single residue substitutions on TolAIII^{Vc}. We confirmed that the different TolAIII^{Vc} variants showed production level and stability equivalent to the wild-type T18-TolAIII construct by immunodetection (Fig. 3*B*), and we tested their capacity to interact with T25-pIII-N1 in a Oxi-BTH assay (Fig. 3*C*). The TolAIII(K324E) and TolAIII(R325D) mutants were, respectively, partially and totally impaired in their ability to interact with pIII-N1^{CTX}, whereas the TolAIII(K347E) mutant retained its ability to bind pIII-N1^{CTX}. Conversely, we introduced the mirror mutations on T25-pIII-N1^{CTX} to generate the E37Q/D39N and the E92K variants. We demonstrated that T25-pIII-N1(E37Q/D39N) was unable to bind T18-TolAIII^{Vc}, although T25-pIII-N1(E92K) was. Together, these data suggested that the two intermolecular salt bridges engaged between Lys-324 and Arg-325 on TolAIII^{Vc} and Glu-37 and Asp-39 on pIII-N1^{CTX} are crucial for pIII-N1–TolAIII^{Vc} complex stabilization.

To confirm the role of the TolAIII charged patch (Lys-324–Arg-325) in pIII-N1^{CTX} binding, we swapped the charged residues engaged into salt bridges between the two partners. As predicted, the T18-TolAIII(K324E/R325D) double mutant was not able to interact with the wild-type T25-pIII-N1^{CTX} construct but regained interaction with the mutated variant presenting oppositely charged residues T25-pIII-N1(E37K/D39R) (Fig. 3*C*). Of note, the restored interaction signal appeared weaker than the one observed for wild-type constructs, possibly reflecting that additional local steric effects operate at the binding interface.

To further establish that our data result from a specificity of interaction rather than a folding defect of the protein variants, we developed an NMR approach. We used the pIN3-ompA2 vector (33) to overproduce ^{15}N-labeled wild-type pIII-N1^{CTX}, pIII-N1^{CTX}(E37Q/D39N), and pIII-N1^{CTX}(E92K) variants fused to a His C-terminal tag. The ^{1}H-^{15}N HSQC spectra of the proteins (Fig. 4, *A*, *C,* and *E*) shows ^{15}N/^{1}H correlations for the

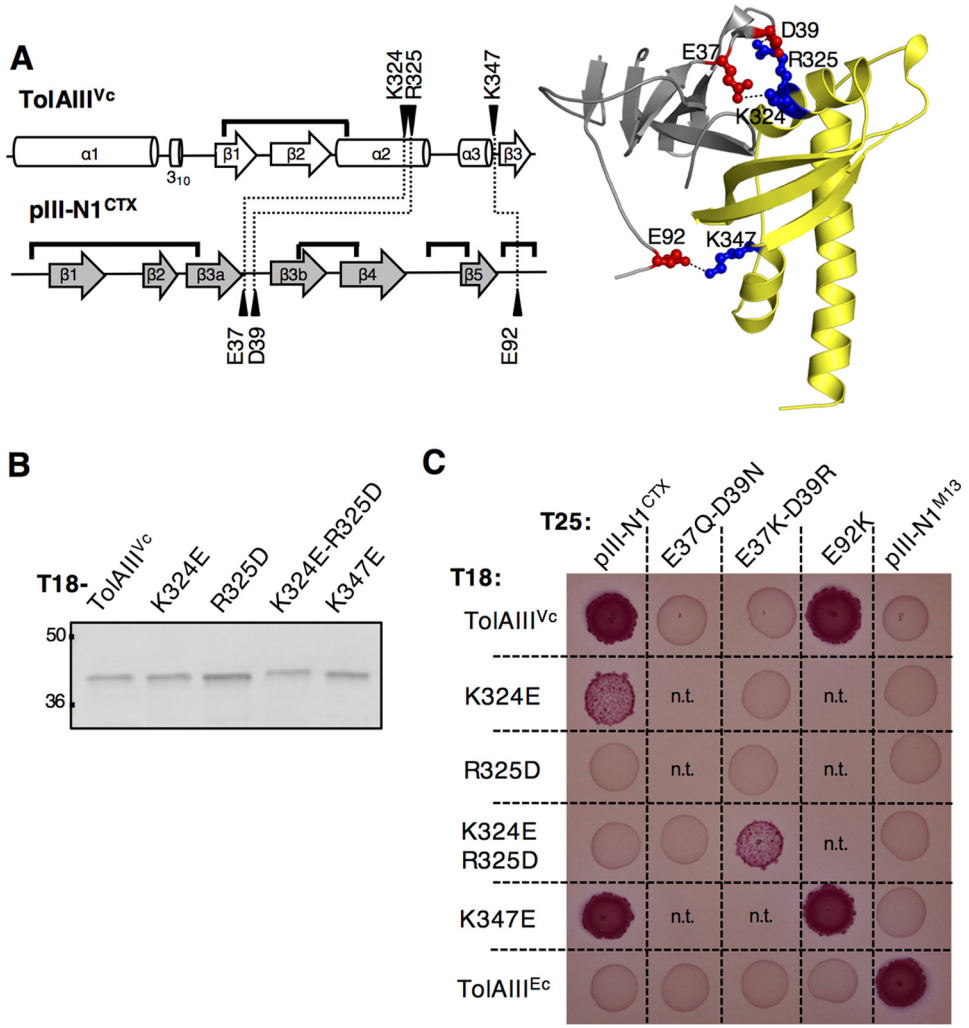

Figure 3. pIII-N1^{CTX}-TolAIII^{Vc} binding relies on two salt bridges. *A, left,* schematic representation of the *V. cholerae* TolAIII and CTX phage pIII-N1 secondary structure. Residues (*black arrowheads*) engaged into intermolecular salt bridges (*dotted lines*) and disulfide bonds (*black lines*) are pointed out. *Right,* X-ray structure of the complex showing the three key salt bridges. *B,* Western immunoblot of 0.2 absorbance units of whole-cell lysates of *E. coli* DH5α strain carrying T18-TolAIII^{Vc} construct, or variants of interest, and probed with anti-T18 antibody. The molecular mass markers (in kDa) are indicated on the *left. C,* TolAIII^{Vc} and pIII-N1^{CTX} point mutants were tested for their binding ability, in comparison with the wild-type constructs, in an Oxi-BTH assay on MacConkey plates. TolAIII^{Ec} and pIII-N1^{M13} are used as a controls. *n.t.,* not tested.

NH group of each amino acid of the proteins. The ^{15}N and ^{1}H resonances are associated with the nuclear chemical environment; thus, the ^{1}H-^{15}N HSQC spectrum represents the fingerprint of a protein. In the case of the native and variant pIII-N1^{CTX}, the ^{1}H-^{15}N HSQC spectra are well resolved. This indicates that each residue has a particular environment in agreement with the X-ray structure of the protein (15). The fact that the spectra of the variant proteins are similar to that of the native protein demonstrates the conservation of the folding. Moreover, superimposition ^{1}H-^{15}N HSQC in the presence and the absence of TolAIII^{Vc} showed chemical shift perturbations for pIII-N1^{CTX} (Fig. 4*B*) and pIII-N1^{CTX}(E92K) variants (Fig. 4*D*), whereas no perturbation was seen with the pIII-N1^{CTX}(E37Q/D39N) variant (Fig. 4*F*). These observations demonstrate that pIII-N1^{CTX} and pIII-N1^{CTX}(E92K) could interact with the TolAIII^{Vc} domain, modifying the chemical environment of the nucleus located at the interface, whereas the pIII-N1^{CTX}(E37Q/D39N) variant could not, which confirmed the Oxi-BTH results.

In V. cholerae, periplasmic expression of the CTX pIII-N1 domain leads to Tol phenotypes

Oxi-BTH assay and NMR studies allowed us to identify key residues on the CTXΦ minor capsid protein that were involved in TolAIII binding. To confirm these data *in vivo*, we used a periplasmic expression assay in *V. cholerae*. In *E. coli*, it has been previously shown that production of the N-terminal domain of colicin A (34) or of the pIII-N1 domain of coliphage f1 (10) into the periplasm of WT cells perturbs the Tol-Pal system by sequestering the TolA protein, and consequently results in *tol* phenotypes. This approach is particularly suitable to study the translocation step of phage infection, as it does not require production and assembly of mutated phage particles, their TCP-dependent reception, and their OM transport.

We used the pIN3-ompA2 vector to express the His-tagged pIII-N1^{CTX} wild-type sequence (or variants) fused to a N-terminal *ompA* signal sequence to allow transport of the produced

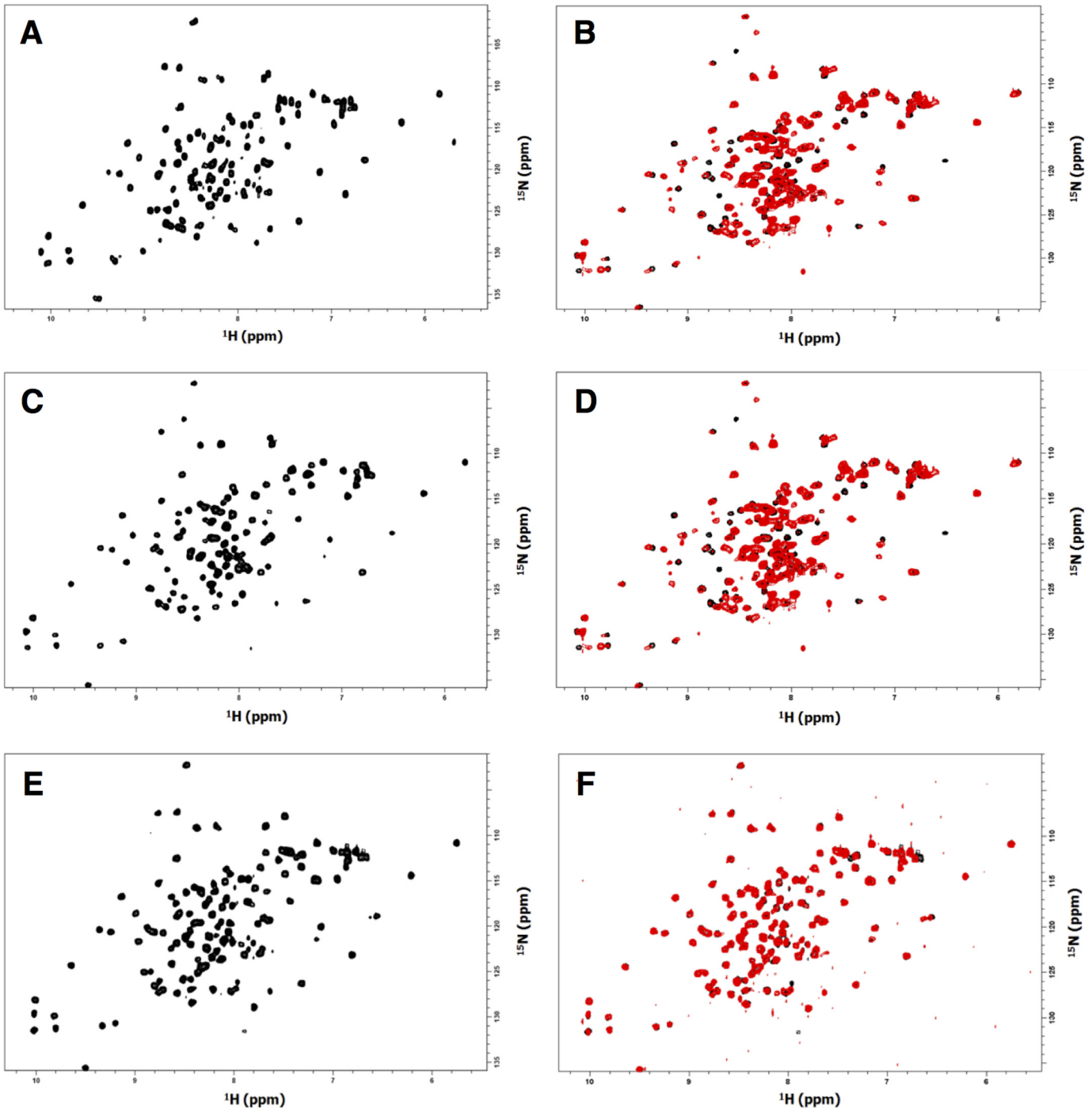

Figure 4. *A*, ^{1}H-^{15}N HSQC of ^{15}N-labeled pIII-N1^{CTX} domain. *B*, ^{1}H-^{15}N HSQC of ^{15}N-labeled pIII-N1^{CTX} domain in the absence (*black*) and in the presence of TolAIII^{Vc} domain (*red*). *C*, ^{1}H-^{15}N HSQC of ^{15}N-labeled pIII-N1^{CTX} (E92K) domain. *D*, ^{1}H-^{15}N HSQC of ^{15}N-labeled pIIIN1^{CTX}(E92K) domain in the absence (*black*) and in the presence of TolAIII^{Vc} domain (*red*). *E*, ^{1}H-^{15}N HSQC of ^{15}N-labeled pIIIN1^{CTX}(E37Q/D39N) domain. *F*, ^{1}H-^{15}N HSQC of ^{15}N-labeled pIIIN1^{CTX}(E37Q/D39N) domain in the absence (*black*) and in the presence of TolAIII^{Vc} domain (*red*).

proteins into the periplasm via the sec pathway. Correct production of the resulting proteins in *V. cholerae* cells was confirmed by immunodetection, whereas transport of the produced domains into the periplasm was attested by sodium azide inhibition of the sec pathway (supplemental Fig. S2). Cells producing the WT pIII-N1 phage domain targeted to the periplasm presented a 5-fold decrease in susceptibility to phage infection (Fig. 5*A*) and high sensitivity to deoxycholate (DOC) (Fig. 5*B*) and to SDS (Fig. 5*C*), which are characteristic *tol* phenotypes. This suggests that the exogenous pIII-N1^{CTX} domain interacts with the endogenous TolA^{Vc} protein in the *V. cholerae* cell envelope, competing with the other Tol proteins of the system and preventing adequate functioning that ensures membrane integrity and permits phage uptake. We also observed that exogenous production of pIII-N1^{M13} in *V. cholerae* periplasm does not result in *tol* phenotypes, which demonstrates further that the M13Φ capsid protein pIII does not bind *V. cholerae* TolA protein. In accordance with the Oxi-BTH results,

A

O395 + pIN vector	Frequency of infection	SD	Infection efficiency
empty	7.4×10^{-3}	1.1×10^{-3}	100%
CTX pIII-N1	9.8×10^{-4}	2.9×10^{-4}	13%
E37Q D39N	7.9×10^{-3}	6.3×10^{-4}	107%
E92K	1.1×10^{-3}	2.8×10^{-4}	15%
M13 pIII-N1	6.4×10^{-3}	8.3×10^{-4}	87%

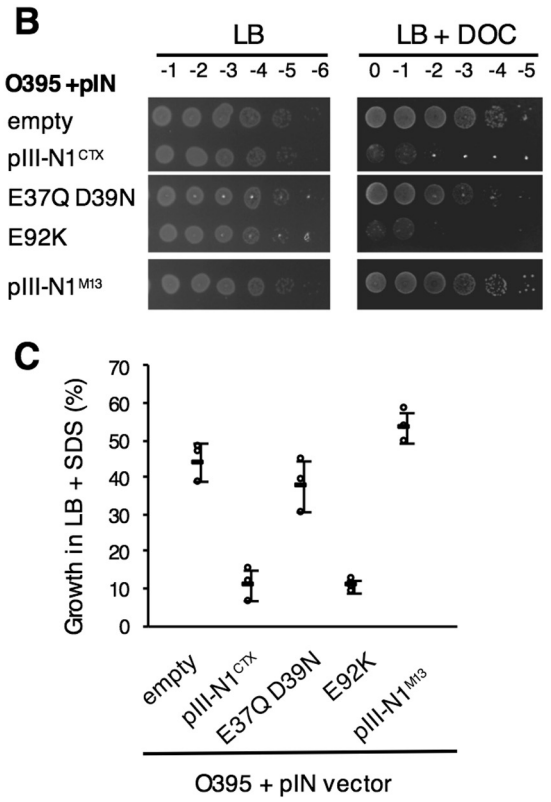

Figure 5. Periplasmic production of CTXΦ pIII-N1 domain or variants in *V. cholerae* and phenotypic characterization. Precultures of *V. cholerae* O395 cells carrying various pIN constructs were grown in LB supplemented with $MgCl_2$ to promote OM integrity and cell growth. *A,* CTX transduction assay was conducted in triplicate, and CFU were counted on LB or LB supplemented with Cm. Frequency of infection is calculated by dividing the number of transductants (CmR colonies) by the number of O395 recipients. The mean and the standard deviation of the triplicate is presented. For each construct, infection efficiency is expressed as the percentage of infection compared with the receiver strain carrying the empty vector. *B,* membrane integrity assay. 4 μl of 10-fold dilution of normalized cultures (initial $A_{595} = 1$) were spotted on LB+amp plates alone or supplemented with 1% DOC. *C,* percentage of survival to SDS 0.125% of the different strains compared with *V. cholerae* WT strain carrying a pIN empty vector. For each strain, percentage of growth is calculated as $A_{600\ nm}$ of each stain grown in LB+SDS $\times$ 100/$A_{600\ nm}$ of the WT strain carrying an empty vector and grown in LB. The experiments were conducted in triplicate, and the standard deviation is presented.

periplasmic expression of the pIII-N1^{CTX}(E37Q/D39N) construct resulted in phage infection rate, DOC sensitivity, and SDS sensitivity similar to the control cells carrying an empty vector, whereas periplasmic expression of the pIII-N1^{CTX}(E92K) variant showed the same phenotypes as those obtained with the WT pIII-N1^{CTX} construct. In accordance with the Oxi-BTH results, these *in vivo* data confirm that the pIII-N1^{CTX} negatively charged residues Glu-37 and Asp-39 are required for pIII-N1 interaction with the native TolA protein.

Evidence that TolA Arg-325 residue is essential for proper functioning of the Tol-Pal system in V. cholerae

We decided to investigate whether the TolA charged patch (Lys-324–Arg-325) required for phage binding is important for the Tol-Pal system function in *V. cholerae*. Although multiple attempts to delete the *V. cholerae* full-length *tolA* gene by double homologous recombination were unsuccessful, we found that a TolAΔ(41–421) mutant, deleted for its periplasmic domains but retaining its IM domain, is viable. The resulting strain presents characteristic *tol* phenotypes (6, 35), including resistance to CTXΦ infection, sensitivity to SDS and to DOC, and finally growth defect in a low osmolarity medium (tryptone broth, 66 mM NaCl) compared with LB medium (Fig. 6, *A–E*).

We first performed a complementation assay of the TolAΔ(41–421) mutant using a pBAD expression vector. TolA has been reported to be a low abundance protein (400–800 copies in *E. coli* cells (36)). In our assay, basal level of TolA production from the pBAD-TolA vector was detected even in the absence of induction (Fig. 6*A*), and it was sufficient to almost fully complement (80–100% rescue) the *V. cholerae tolA* mutant for phage infection (Fig. 6*B*), for resistance to SDS and DOC (Fig. 6, *C* and *D*), and for hypo-osmotic growth in tryptone broth (Fig. 6*E*). These results also confirmed that the deletion had no polar effect on the other genes of the Tol-Pal operon.

We then tested *V. cholerae* strains carrying TolA variants where residues Lys-324, Arg-325, or Lys-347 were mutated for oppositely charged residues. Although the K324E variant behaved similarly to the wild-type pBAD-TolA construct, rescue was no longer observed for the TolA(R325D) variant, despite adequate production of the mutant protein (Fig. 6, *A–E*). The TolA(K324E/R325D) double mutant showed a slightly stronger phenotype than the individual mutants for membrane integrity assays (Fig. 6, *C* and *D*). Finally, the TolA(K347E) variant complemented the mutant strain similarly to the WT TolA construct. Together, these findings support the conclusion that the positively charged residue Arg-325 plays a dominant role in TolA function in *V. cholerae*, whereas Lys-324 and Lys-347 do not.

Conservation of the Lys-324 and Arg-325 residues in other TolA Vibrio species

The Tol-Pal system has a widespread distribution in Gram-negative bacteria. We first questioned TolA sequence conservation among 128 *V. cholerae* isolate genomes available on the NCBI database, and we found that the full-length protein is 100% identical (supplemental Fig. S3). We then broadened the study to the Vibrionaceae family, including 82 *Vibrio* species (supplemental Fig. S4) and 33 non-*Vibrio* species (six *Aliivibrio*, three *Enterovibrio*, five *Grimontia*, 13 Photobacterium, and six *Salinovibrio* (supplemental Fig. S5). PSIPRED analysis (37) of the TolAIII amino acid sequences suggests that the secondary structures are conserved among Vibrionaceae (data not shown). Alignments of TolAIII sequences from multiple *Vibrio* species indicates that Lys-324 is highly conserved (73/82

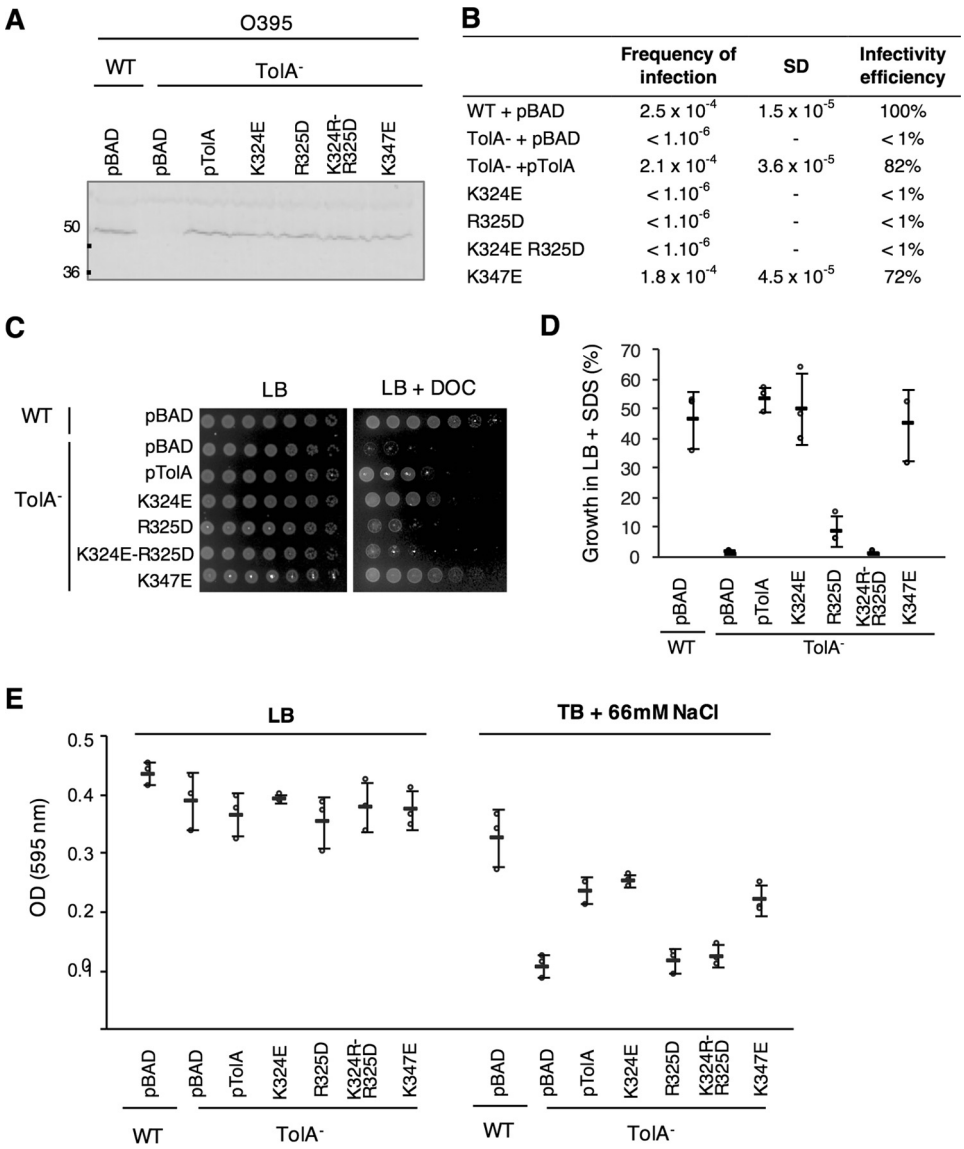

	Frequency of infection	SD	Infectivity efficiency
WT + pBAD	2.5×10^{-4}	1.5×10^{-5}	100%
TolA- + pBAD	$< 1.10^{-6}$	-	< 1%
TolA- +pTolA	2.1×10^{-4}	3.6×10^{-5}	82%
K324E	$< 1.10^{-6}$	-	< 1%
R325D	$< 1.10^{-6}$	-	< 1%
K324E R325D	$< 1.10^{-6}$	-	< 1%
K347E	1.8×10^{-4}	4.5×10^{-5}	72%

Figure 6. Phenotypic characterization of *V. cholerae* O395 WT and TolA$^-$ strains complemented with TolA variants of interest. *A,* expression of the different pBAD-TolA^{Vc} constructs in *V. cholerae* was assessed by Western immunoblotting. A total of 0.3 absorbance units of whole-cell lysate were loaded onto an SDS-13.5% acrylamide gel and immunodetected using polyclonal antibody raised against *E. coli* TolA. *B,* CTX transduction assays were conducted in triplicate, and CFU were counted on LB or LB supplemented with Cm. Frequency of infection is calculated by dividing the number of transductants (CmR colonies) by the number of O395 recipients. The mean and the standard deviation of the triplicate is presented. For each construct, infection efficiency is expressed as the percentage of infection compared with the receiver strain carrying the empty vector. *C,* membrane integrity assay. 4 μl of 5-fold dilution of normalized cultures (initial $A_{600} = 1$) were spotted on LB+kanamycin plates alone or supplemented with 1% DOC. *D,* percentage of survival to SDS-0.125% of the different strains compared with *V. cholerae* WT strain carrying an pBAD empty vector. For each strain, percentage of growth is calculated as $A_{600\ nm}$ of each stain grown in LB+SDS $\times$ 100/$A_{595\ nm}$ of the WT strain carrying an empty vector and grown in LB. *E,* quantification of *V. cholerae* O395 WT and TolA$^-$ mutant growth in LB (407 mOSM) and in tryptone broth (*TB*) supplemented with 66 mM NaCl (123 mOSM). The experiment was conducted in triplicate, and the *error bars* report standard deviations.

sequences) with only few variants where it is replaced by another positively charged residue, arginine (6/82). Three exceptions were found with *Vibrio breoganii*, *Vibrio gazogenes,* and *Vibrio rhizosphaerae* that carry an uncharged glutamine residue at position 324. Overall, the positive charge at position 324 appears to be conserved in other Vibrionaceaes tested (31/33), suggesting its importance in TolA function (supplemental Figs. S4 and S5). Conversely, the positively charged residue Arg-325 is less conserved in *Vibrio* species (51/82), frequently being replaced by the uncharged residue serine (25/82) or less frequently by alanine, threonine, or valine (6/82). Notably, the positively charged residue at position 325 was never observed in other Vibrionaceae species (0/33).

As we previously demonstrated that pIII-N1^{CTX} interaction with the *V. cholerae* TolA receptor is driven by two intermolecular salt bridges engaging TolA Lys-324 and Arg-325 residues, we expected orthologous TolAIII sequences carrying the charged patch (Lys-324–Arg-325) to also be able to bind CTX pIII-N1. As shown in Fig. 7*A*, the TolAIII domain from *Vibrio anguillarum*, *Vibrio tasmaniensis*, and *Vibrio alginolyticus* carry the (KR) patch, whereas *Vibrio harveyi* has a (KS) motif and the Vibrionaceae *Aliivibrio fischeri* has a (KT) motif. The

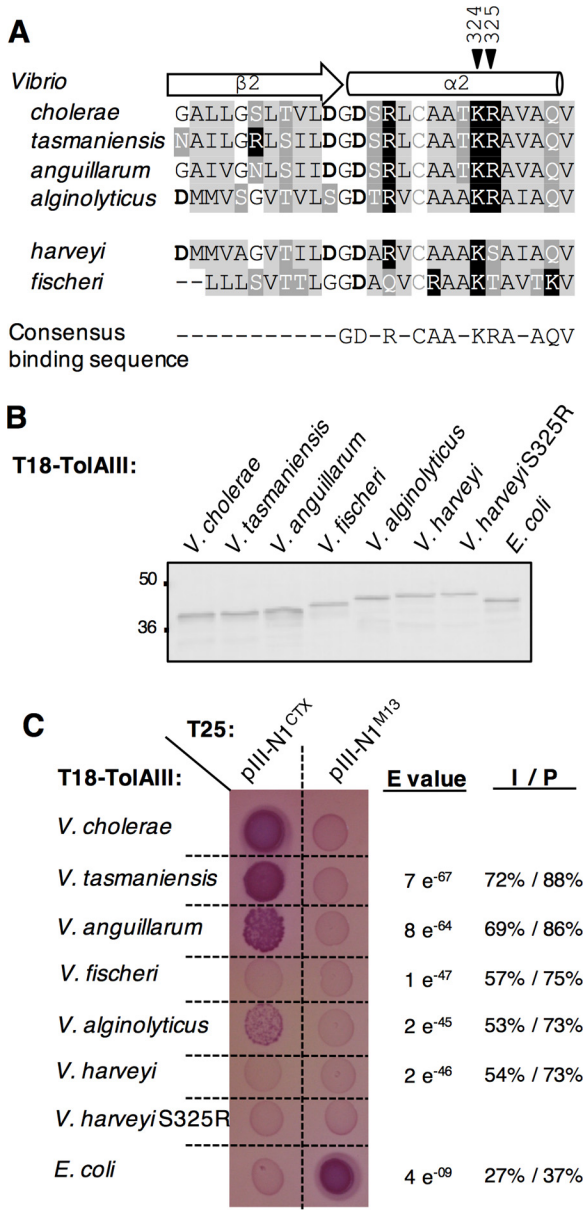

Figure 7. Conservation of TolA Lys-324 and Arg-325 residues in other *Vibrio* species. *A,* sequence alignment between *V. cholerae*, *V. tasmaniensis*, *V. anguillarum*, *V. alginolyticus*, *V. harveyi*, and *V fischeri* TolAIII β2-α2 domain. Residues are colored as follows: basic (*black squares*), acidic (*bold*), hydrophobic (*light gray*),and polar uncharged (*dark gray*). *Black arrowheads* point the Lys-324–Arg-325 motif. *B,* Western immunoblot of 0.2 absorbance units of whole-cell lysates of *E. coli* DH5α strain carrying T18-TolAIII construct from selected Vibrionaceae and from *E. coli* and probed with anti-Cya antibody. The molecular mass markers (in kDa) are indicated on the *left*. *C,* T18-TolAIII constructs from selected species were tested for their binding ability to the T25-pIII-N1^{CTX} in an Oxi-BTH assay on MacConkey plates. *E. coli* TolAIII and pIII-N1^{M13} are used as a controls. Sequence comparison between each TolAIII of interest and the *V. cholerae* TolAIII amino acid sequences using Blast2 is reported on the *right* of the panel as E value, identity (*I*) and positive (*P*) values.

TolAIII coding sequences from the different species were cloned into the pUT18 vector, and correct expression of the different constructs was assessed by immunodetection (Fig. 7*B*) before testing their interaction ability with T25-pIII-N1^{CTX} in the Oxi-BTH assay. As shown on Fig. 7*C*, T18-TolAIII from *V. anguillarum*, *V. tasmaniensis*, and *V. alginolyticus* showed positive interaction signal with T25-pIII-N1^{CTX}. In contrast, T18-TolAIII$^{V. harveyi}$ and T18-TolAIII$^{V. fischeri}$, lacking the positively charged patch (KR), were not able to bind pIII-N1^{CTX}. We analyzed the TolAIII sequences that were able to bind pIII-N1 to define a consensus sequence for partner recognition. We found that TolAIII tolerates multiple sequence variation in the β2-strand, likely because this region of the protein interacts with pIII-N1 β1-strand through backbone hydrogen bond interactions. Conversely, TolAIII α2-helix alignments allowed the definition of a consensus sequence (GD(S/T)R(L/V) CAA(T/A)KRA(V/I)AQ) surrounding the (KR) residues. We noticed that *V. harveyi* TolAIII carry the defined consensus sequence, apart from Arg-325. However, point mutation to generate T18-TolAIII$^{V. harveyi}$ S325R and reconstitute a positively charged patch (KR) was not sufficient to restore interaction with pIII-N1^{CTX} (Fig. 7*C*).

Discussion

New in vivo protein–protein interaction assay dedicated to disulfide-oxidized proteins

For many proteins functioning in the periplasm, exposed at the cell surface, or secreted in the extracellular environment, stability and/or activity require the formation of disulfide bonds. For example, in *V. cholerae*, S–S bond proteins include the cholera toxin (38), the pilin subunits that assemble in different type IV pili (TCP, MshA, and PilA) operating into the various aspects of *Vibrio* ecology (39, 40), the TolA protein in the Tol-Pal complex involved in envelope integrity and cell division (15), and sensors such as TcpP (41, 42) and ToxR (43) operating signal transduction to regulate virulence pathways. Thus, identification and characterization of physiologically relevant interactions between these S–S bond proteins *in vivo* are crucial tasks for the understanding the molecular processes within the cell.

The original BACTH approach is an easy yet efficient technique that has become a common laboratory tool used to identify and dissect protein/protein interactions (29, 44). As the interaction between candidates of interest is tested in the cell cytoplasm, studies were restricted so far to proteins in their reduced state. Recently, the development of new BACTH plasmids inserting a transmembrane segment downstream of the T25 and T18 fragments was shown to allow the detection of interactions occurring within the periplasmic space of the cell (45).

In this study, we extended the range of BACTH application to the study of disulfide-oxidized proteins directly in the reporter cell cytoplasm thanks to a new genetic background that we named Oxi-BTH. In this strain, correct disulfide reshuffling is catalyzed by a cytoplasmic version of the disulfide bond isomerase DsbC (31). The Oxi-BTH assay was validated by the visualization of interactions previously described between proteins with unique (TolAIII^{Ec} and TolAIII^{Vc}) and multiple disulfide bonds (pIII-N1^{M13} and pIII-N1^{CTX}), which could not be observed in the regular BACTH assay. As a protein with eight cysteines, pIII-N1^{CTX} has a probability of less than 1% to form the correct four disulfide bonds, and our results also attest the efficiency of the cytoplasmic DsbC proofreading activity (Fig. 1). Finally, this tool was suitable to individually test the importance of each disulfide bond and of targeted residues in protein/

protein interactions (Figs. 2 and 3). Many BACTH pUT18 and pKT25 constructs have already been published, and genome-wide libraries are available for *E. coli* (46) and *Pseudomonas aeruginosa* (47) allowing the constitution of a large collection of potential partners that can be directly tested in the Oxi-BTH assay without requiring new cloning steps. In this context, we believe that Oxi-BTH constitutes a robust and versatile tool to test the importance of oxidative folding in protein/protein interaction, to identify key amino acids involved, and to investigate the specificity of binding between two proteins of interest.

Refining the model of CTXΦ uptake

Filamentous phage infection is a two-step process, requiring a primary receptor at the surface of the cell (the TCP pilus in the case of CTXΦ) and a secondary receptor, TolA, inside the cell envelope. In this study, our aim was to gain insight into the second step of the infection process by investigating *in vivo* the phage/TolA interaction. In contrast to *E. coli*, we did not manage to obtain the *V. cholerae* TolA clean deletion mutant by homologous recombination, although we were able to delete the periplasmic domains of the protein. It is noteworthy that the only other *V. cholerae* TolA^{-} mutant published in the literature is a *tolA*::*pGP704* disruption mutant (obtained by single crossover) that, according to the primer design, also resulted in a truncated TolA protein somewhere in the periplasmic domain (6). This suggests that, under laboratory conditions, TolA is essential in *V. cholerae*, as reported previously in *E. coli* O7:K1 (48), *P. aeruginosa* (49), and *C. crescentus* (26), but is dispensable in the *E. coli* K12 strain (35).

We observed that pIII-N1^{CTX} domain is sufficient for TolA binding and that pIII-N2^{CTX} does not impede the interaction between the two partners (Fig. 2). This result is in agreement with previous observations made by Ford et al. (15). Indeed, the authors previously showed that CTXΦ incubation with an excess of purified TolAIII^{Vc} domain before infection of *V. cholerae* O395 cells reduced the infection efficiency. However, in this study, binding between pIII-N1-N2^{CTX} and TolAIII^{Vc} had not been formally tested because pIII-N1-N2^{CTX} could not be purified in a soluble form (15). Together, our data further demonstrate that the CTXΦ naturally exposes a TolA-binding site on the N-terminal domain of pIII, which is reminiscent to IF1 and IKe coliphage infection strategy (50). It implies that CTXΦ binding to the primary receptor TCP might be responsible for phage recruitment from the environment and possibly active pulling to the cell surface through retraction (14), but it is not required to unmask the pIII-N1 TolA-binding site.

The crystal structure of the complex (PDB code 4G7X) suggested that multiple interactions (ionic, hydrophobic, polar contacts, and van der Waals forces) contribute to the binding interface between TolAIII^{Vc} and pIII-N1^{CTX}. The TolAIII^{Vc} β2-strand folds around pIII-N1^{CTX}, resulting in a continuous intermolecular β-sheet that involves multiple hydrogen bonds between the backbone chains of TolAIII β2-strand and pIII-N1 β1-strand. TolAIII^{Vc} residues Lys-324, Arg-325, and Lys-347 form three salt bridges with pIII-N1 Glu-37, Asp-39, and Glu-92 residues, respectively (Fig. 3). However, the contribution of each of the individual interactions in the TolAIII–pIII^{CTX} complex formation cannot be assessed from the crystal structure. By combining *in silico* analysis and *in vivo* experimental data, we defined that the consensus sequence for CTX binding on TolAIII^{Vc} is restricted to the α2-helix, whereas the β2-strand tolerates multiple residues variations (Fig. 7). Moreover, our work clearly demonstrates that the two salt bridges engaged between TolAIII^{Vc} residues Lys-324 and Arg-325, and CTX phage pIII-N1 residues Glu-37 and Asp-39, respectively, provide the driving forces of the interaction, forming ion locks required for the complex to form, whereas the TolAIII Lys-347–pIII-N1 Glu-92 bond is dispensable. It is noteworthy that mutating the TolAIII Arg-325 residue alone had a stronger negative impact on phage binding than mutating the TolAIII Lys-324 residue (Fig. 3). We used the 2P2I database (http://2p2idb.cnrs-mrs.fr/2p2i_inspector.html)[4] (51, 52) to gain insights into the protein–protein interface parameters. Results showed a total of 88 non-bonded contacts (distance cutoff 4 Å) between pIII-N1^{CTX} and TolAIII^{Vc} (supplemental Fig. S4). Among these 88 contacts, TolAIII Arg-325 was engaged in 20 different contacts with pIII-N1 surface, whereas TolAIII Lys-324 was engaged in six (supplemental Fig. S6). These observations might explain the more predominant role of the TolAIII Arg-325 residue in pIII-N1 binding, compared with Lys-324. Overall, this is reminiscent of what was previously observed for M13 coliphage pIII-N1 binding on the concave side of TolAIII^{Ec}, where the interaction makes an antiparallel continuous β-sheet stabilized by two salt bridges (TolAIII^{Ec} Asp-210, Lys-212 interacting with pIII-N1^{M13} Arg-29 and Asp-28, respectively (PDB code 1Tol (8)). It would be interesting to test the importance of each of these ionic interactions for coliphage–TolA^{Ec} complex formation.

TolA is involved in the fitness of *V. cholerae*, in particular in low osmolarity conditions, such as those found when the bacterium reaches low salinity environments (fresh water), or in response to detergent components, such as the bile acid deoxycholate during its transit through the gastrointestinal track (Figs. 5 and 6) (6). We found that the TolA(R325D) variant was functionally unable to complement the *V. cholerae tol* mutant, whereas the TolA(K324E) mutant was able to do so (Fig. 6). We questioned the sequence conservation of TolAIII in other *Vibrio* species, but we did not observe strict correlation between conservation of the Lys-324 and Arg-325 residues and their importance in TolA function in the tested conditions. Interestingly, we noticed that in the 33 Vibrionaceae species studied, the TolAIII Arg-325 residue is absent (supplemental Fig. S3), whereas additional positive charges are found at more or less one pitch of the α2 helix: Arg-321 (occurrence 33/33) and Lys-329 (occurrence 24/33). Because TolA is a hub protein, and part of a multicomponent complex, the patch of positive residues on the α2 helix might be involved in partners binding, either with an already known partner of the TolAIII domain such as TolB or Pal (16, 22, 53) or an unknown partner that still has to be identified.

We demonstrated that the KR patch on TolA is crucial but not sufficient for CTX binding (Fig. 7). Indeed, study of the

[4] Please note that the JBC is not responsible for the long-term archiving and maintenance of this site or any other third party hosted site.

V. harveyi TolA(S325R) variant suggests that additional local steric effects operate at the binding interface, outside the α2 helix. Although salt bridges provide the forces to drive protein–protein initial attraction, subsequent complex stabilization is usually the result of cooperative interactions that encompass multiple pairwise bonds (54). Our results allow a better understanding of the TolAIII/pIII-N1 interaction interface, with two salt bridges providing the driving forces of the interaction, whereas the formation of the intermolecular anti-continuous β-sheet provides stabilization interactions to the complex. By targeting important functional and/or conserved residues of TolA protein, CTXΦ uses a parasite infection strategy that may help to prevent *V. cholerae* from escaping the infection.

Implication for the CTX infection host specificity

In this work, we observed that the CTX phage protein pIII-N1 responsible for host selection (5) can bind the TolAIII receptor domain from at least three other *Vibrio* species: *V. alginolyticus*, *V. anguillarum,* and *V. tasmaniensis* (Fig. 7). However, the host range reported for CTX from environmental sampling studies is surprisingly narrow, even in species carrying a conserved TolA sequence. Thus, although all the epidemic *V. cholerae* strains belonging to the O1 or O139 serogroups carry the CTX prophage, it is rarely detected (2–5%) in non-O1/non-O139 *V. cholerae* environmental isolates genomes (55–59). Apart from *V. cholerae*, CTXΦ has been reported to infrequently infect other *Vibrio* species, even for very close species such as *Vibrio mimicus* (60). It has been proposed that the limited distribution of the primary receptor TCP among *Vibrio* species plays a predominant role in the fate of the entire infection process (55). It is interesting to note that TCP-independent CTXΦ infection has been reported to occur in defined conditions (5). Thus, whereas TolA is a conserved protein, variation in the sequence of the TolAIII domain might serve as a second level of CTXΦ host-specificity checkpoint.

Because bacteriophages, like any other viruses, are obligate intracellular parasites, successful uptake across the bacterial cell envelope is an essential condition to complete their life cycle. However, current knowledge on host/phage interactions is based on a limited number of microbial models. This scientific problem outreaches the question of *V. cholerae* pathogenic conversion, as other filamentous phages (sharing similarities with CTXΦ) have been demonstrated to affect the virulence and fitness of a large range of bacterial hosts: meningococcal disease-associated (MDA) phage in invasive isolates of *Neisseria meningitidis* (61); YpfΦ in the plague bacillus *Yersinia pestis* (62); and CUS-1 in the high-virulence clone *E. coli* O18:K1:H7 (63). In this context, our work emphasizes the necessity to study CTXΦ infection on its own and to overtake the Ff coliphage model of infection. It also sheds light on the mechanism underlying the initial filamentous phage–bacterial host binding and provides basic knowledge that might serve the understanding of transduction-dependent spreading of virulence factors in bacterial populations.

Experimental procedures

Bacterial strains and growth conditions

Relevant bacterial strains and plasmids used in this study are listed in supplemental Table S1. Bacteria were routinely cultivated in Luria-Bertani broth (LB, 407 mosM) at 37 °C (*E. coli*) or 30 °C (*V. cholerae*). When specified, $MgCl_2$ (2 mM) was added to the culture medium to promote OM integrity and cell growth of *tol* mutants. Tryptone broth (1% (w/v) tryptone, 66 mM NaCl, pH 8.5) was used as a low osmolarity medium (123 mosM (64)). When indicated, antibiotics were added to the medium at the following concentrations: streptomycin (100 μg/ml); ampicillin (50 or 100 μg/ml); kanamycin (50 μg/ml); chloramphenicol (30 μg/ml for *E. coli* and 1 μg/ml for *V. cholerae*). *V. cholerae tolA* Δ(41–421) in-frame deletion mutant was constructed as described previously using the primers listed in supplemental Table S2 and the suicide plasmid pWM91 (65, 66). The absence of the TolA protein in the mutant strain was confirmed by Western blotting using polyclonal antibodies directed against *E. coli* TolAII-III protein (30) and cross-reacting with TolAIII^{Vc}.

Plasmid construction

Polymerase chain reactions (PCR) were performed using Q5 High Fidelity DNA polymerase (New England Biolabs). Primer sets required to generate genetic constructs were synthesized by Sigma (supplemental Table S2). Enzymes (New England Biolabs) were used according to the manufacturer's instructions. Plasmids have been constructed either by standard restriction/ligation protocol, by Sequence and Ligase Independent Cloning (SLIC) (67) as modified by Jeong *et al.* (68), or by restriction-free cloning as described previously (69). Briefly for restriction-free cloning, genes of interest were amplified with oligonucleotides introducing extensions annealing to the target vector. The double-stranded product of the first PCR has then been used as oligonucleotides for a second PCR using the target vector as template and *Pfu* Turbo polymerase (Stratagene, La Jolla, CA). For BACTH plasmid constructs, the *V. cholerae* El Tor N16961 genome was used as a template to PCR-amplify the pIII^{CTX}-encoding gene (*orfU*, at loci vc1460). The *tolA* sequence was amplified from *V. cholerae* O395 (locus VC0395_A1430) or from *E. coli* W3110 (locus BL257_RS03625) genomes. The pG3 vector (10) was used as a template to amplify pIII^{M13}. Amplified products were cloned into a pUT18c or a pKT25 expression vector (29) to generate fusions with the adenylate cyclase T18 and T25 domains. For construction of the pBAD-TolA rescue plasmid, the native sequence of *V. cholerae* O395 TolA, retaining the start and the stop codons, was amplified by PCR. The forward primer was designed to introduce a Shine-Dalgarno consensus sequence GAAGGAGATATACATACCC directly upstream of the start codon. The amplification product was then introduced into the pBAD18-Kan vector (70). For periplasmic expression, pIN-pIII-N1^{CTX} plasmid was constructed by PCR-amplifying the pIII-N1^{CTX} sequence (without start codon) with an upstream oligonucleotide encoding Strep-tag II (WSHPQFEK) and a downstream oligonucleotide encoding a C-terminal His_6 sequence. Digestion of the PCR product and the pIN-ompA2

vector (33) with EcoRI and BamHI enzymes allowed subsequent ligation of the PCR product into the vector. The pIN-PIII-N1^{M13} plasmid (previously named pG3) has been described previously (10).

Mutations on pUT18-TolA, pKT25-pIII-N1, pIN-pIII-N1, and pBAD-TolA plasmids were performed by QuikChange site-directed mutagenesis using complementary pairs of oligonucleotides (listed in supplemental Table S2) and *Pfu* Turbo polymerase. All constructs were confirmed by DNA sequencing (Eurofins, MWG).

Construction of the Oxi-BTH strain

To conduct bacterial two-hybrid experiments in an oxidative environment, the *E. coli* K12 SHuffle T7 strain (New England Biolabs) was engineered further. This initial strain is deleted for glutaredoxin reductase (*gor*) and thioredoxin reductase (*trxB*) genes, which allows disulfide bond formation in the cytoplasm. Moreover, cytoplasmic expression of the disulfide bond isomerase DsbC acts on proteins with multiple disulfide bonds, promoting correct disulfide bond formation and proper folding. In this genetic background, the *cya*° mutation was transduced using a P1 lysate of an *E. coli* K12 *cya*° strain. The resulting mutant strain, named Oxi-BTH, was unable to ferment sugars, and consequently it grew as white colonies when plated on MacConkey plates.

Bacterial two-hybrid assay in E. coli BTH101 and Oxi-BTH strains

The adenylate cyclase-based bacterial two-hybrid technique was used as published previously (29), with the following modifications. Pairs of proteins to be tested were fused to the isolated T18 and T25 catalytic domains of the *Bordetella* adenylate cyclase. After transformation of the two plasmids producing the fusion proteins into the reporter BTH101 or Oxi-BTH strains, plates were incubated at 37 °C for 24 h. Three colonies for each transformation were inoculated into 600 μl of LB medium supplemented with ampicillin, kanamycin, and IPTG (0.5 mM). After overnight growth at 30 °C, 5 μl of each culture were dropped onto MacConkey plates supplemented with ampicillin, kanamycin, and IPTG (0.5 mM). Plates were incubated for 16–24 h (BTH101) and 2–3 days (Oxi-BTH) at 30 °C. The experiments were done at least in triplicate, and a representative assay is shown.

SDS-PAGE and immunoblotting

Protein samples resuspended in 2× loading buffer were subjected to SDS-PAGE. When specified, 2-mercaptoethanol (5% final) was added to the samples. For detection by immunostaining, proteins were transferred onto nitrocellulose membranes, and immunoblots were probed with primary antibodies and goat secondary antibodies coupled to alkaline phosphatase and developed in alkaline buffer in the presence of 5-bromo-4-chloro-3-indolyl phosphate and nitro blue tetrazolium. The anti-TolAIII^{Ec} polyclonal antibodies are from our laboratory collection, and the anti-5 His monoclonal antibody (Qiagen), the anti-CyaA monoclonal antibody (3D1, Santa Cruz Biotechnology), and alkaline phosphatase-conjugated goat anti-rabbit and anti-mouse antibodies (Millipore) have been purchased as indicated.

V. cholerae phenotypic analysis

Sensitivity test to SDS—V. cholerae cells harboring the empty plasmid as a control or the plasmid encoding the constructs of interest were grown in LB medium at 30 °C until stationary phase, then back-diluted to initial $A_{595\ nm} = 0.2$ in LB supplemented or not with 0.125% SDS, and grown for 7 h at 30 °C with agitation. The percentage of surviving cells was estimated from the turbidity ratio of the SDS-treated cells and the control samples. Experiments were performed in triplicates.

Sensitivity test to deoxycholate—Normalized serial dilutions of strains to be tested were spotted onto 1% DOC-supplemented LB plates. After overnight incubation at 37 °C, survival was reported as the highest dilution of strain able to form colonies.

Growth in low osmolarity conditions—The different strains were grown in LB medium at 30 °C until stationary phase, then back-diluted 100-fold in LB medium (osmolarity 407 mOsM) and in tryptone broth (1% (w/v) tryptone, 66 mM NaCl, pH 8.5, 123 mOsM (64)), and incubated for 16 h at 30 °C. The percentage of growth was estimated from the turbidity ratio of the tested strains and the control sample. Experiments were performed in triplicates.

CTX-cm phage particle preparation

The *dif1*$^-$ strain BS2 (71) harboring the chloramphenicol-marked CTX$^{El\ Tor}$ phage replicative form (pCTX-cm) was used as a donor strain to produce CTX phage particles. The donor strain was streaked onto LB-Cm (1 μg/ml) plates and incubated at 37 °C overnight. A single colony was used to inoculate a 2-ml LB + Sm 100 culture and incubated at 37 °C for 16 h. Cell were pelleted by centrifugation, and the supernatant containing phages was filter-sterilized using a 0.22-μm syringe filter. Phage preparation was checked for sterility by plating on an LB plate.

Susceptibility to CTX phage infection assays

Cell susceptibility to phage infection was conducted as described previously (72). Briefly, for each recipient strain three independent clones were cultivated separately in TCP-inducing conditions (LB 1% tryptone, 0.5% yeast extract, 0.5% NaCl, pH 6.5, 30 °C). After 20 h of growth, 75 μl of cells were mixed with 75 μl of CTX-cm phage suspension. The mixture was incubated during 30 min at room temperature without shaking, then 500 μl of LB was added, and the cell suspension was incubated at 37 °C with vigorous shaking for 45 min to allow cell recovery. Then dilutions of the cell suspension were plated on LB agar plates supplemented with Sm (100 μg/ml) or with Sm (50 μg/ml), and Cm (1 μg/ml) to enumerate total cells and transductant cells, respectively. The frequency of infection was determined by dividing the number of transductants by the number of total recipient cells.

NMR spectroscopy

For NMR studies, a TolA(237–356)^{Vc} (TolAIII^{Vc}) construct was included in a plasmid with the gene of OmpA signal sequence for protein secretion at the N terminus and His_6 tag

for the purification at the C terminus. For the native and variant pIII-N1^{CTX}, the OmpA signal sequence and His_6 tag construct were used, with an additional strep tag at the N terminus of the gene sequence. ^{15}N isotopic labeling of native and mutant pIII-N1^{CTX} was obtained from bacteria grown on M9 medium containing 1 g/liter $^{15}NH_4Cl$ as sole source of nitrogen. The proteins were overexpressed in *E. coli* BL21 strain. Protein production was obtained after 2 h of IPTG induction at 37 °C. Protein purification was obtained from periplasmic extract pulled on nickel-nitrilotriacetic acid-agarose and eluted with imidazole step gradient.

NMR spectra were recorded on a Bruker 600 MHz spectrometer equipped with a TCI cryoprobe at 300 K. ^{1}H-^{15}N HSQC spectra were processed with TopSpin software. For NMR experiments pIII-N1^{CTX} wild type and (E37Q/D39N) double mutant, the concentration was 0.16 mM in 50 mM $NaPO_4$, 50 mM NaCl buffer at pH 6.9. In the case of the complexes, the final TolAIII^{Vc} concentration was 0.32 mM.

In silico analysis

Search for *V. cholerae* O395 TolA orthologous sequences was performed with BlastP and restricted to Vibrionaceae species. Multisequence alignments were performed using Clustal Omega (73) and color-coded with JalView2 tool (24). The 2P2I database (51, 52) was used to list all the non-bonded contacts at the complex interface (PDB code 4G7X) with a cutoff distance of 4 Å.

Author contributions—L. H., M. N., F. G., D. D., and R. L. contributed to the design of the study; L. H., R. N., M. N., and F. G. performed experiments. L. H., R. N., M. N., F. G., D. D., and R. L. contributed to data interpretation. L. H. wrote most of the manuscript. All authors approved the final version of the manuscript.

Acknowledgments—We thank François-Xavier Barre, Paula Watnick, Delphine Destoumieux-Gazon, Marie-Stephanie Aschteng, Long-Fei Wu, and Emmanuelle Bouveret for providing useful strains and plasmids. We thank Emmanuelle Bouveret, Eric Cascales, Bérengère Ize, Marlon Sidore, and all the members of the Laboratoire d'Ingénierie des Systèmes Macromoléculaires for helpful discussions and support; Annick Brun, Isabelle Bringer, Moly Ba, Olivier Uderso, and Faniry Raboanarivola for technical assistance; and Octave Uhleure for encouragements. We thank Olivier Bornet at the NMR platform of IMM for NMR time machine necessary for recording NMR spectra.

References

1. Waldor, M. K., and Mekalanos, J. J. (1996) Lysogenic conversion by a filamentous phage encoding cholera toxin. *Science* **272,** 1910–1914
2. Mai-Prochnow, A., Hui, J. G., Kjelleberg, S., Rakonjac, J., McDougald, D., and Rice, S. A. (2015) Big things in small packages: the genetics of filamentous phage and effects on fitness of their host. *FEMS Microbiol. Rev.* **39,** 465–487
3. Rakonjac, J., Bennett, N. J., Spagnuolo, J., Gagic, D., and Russel, M. (2011) Filamentous bacteriophage: biology, phage display and nanotechnology applications. *Curr. Issues Mol. Biol.* **13,** 51–76
4. Holliger, P., and Riechmann, L. (1997) A conserved infection pathway for filamentous bacteriophages is suggested by the structure of the membrane penetration domain of the minor coat protein g3p from phage fd. *Structure* **5,** 265–275
5. Heilpern, A. J., and Waldor, M. K. (2003) pIIICTX, a predicted CTX minor coat protein, can expand the host range of coliphage fd to include *Vibrio cholerae*. *J. Bacteriol.* **185,** 1037–1044
6. Heilpern, A. J., and Waldor, M. K. (2000) CTXΦ infection of *Vibrio cholerae* requires the tolQRA gene products. *J. Bacteriol.* **182,** 1739–1747
7. Deng, L.-W., and Perham, R. N. (2002) Delineating the site of interaction on the pIII protein of filamentous bacteriophage fd with the F-pilus of *Escherichia coli*. *J. Mol. Biol.* **319,** 603–614
8. Lubkowski, J., Hennecke, F., Plückthun, A., and Wlodawer, A. (1999) Filamentous phage infection: crystal structure of g3p in complex with its coreceptor, the C-terminal domain of TolA. *Structure* **7,** 711–722
9. Lubkowski, J., Hennecke, F., Plückthun, A., and Wlodawer, A. (1998) The structural basis of phage display elucidated by the crystal structure of the N-terminal domains of g3p. *Nat. Struct. Biol.* **5,** 140–147
10. Pommier, S., Gavioli, M., Cascales, E., and Lloubès, R. (2005) Tol-dependent macromolecule import through the *Escherichia coli* cell envelope requires the presence of an exposed TolA binding motif. *J. Bacteriol.* **187,** 7526–7534
11. Riechmann, L., and Holliger, P. (1997) The C-terminal domain of TolA is the coreceptor for filamentous phage infection of *E. coli*. *Cell* **90,** 351–360
12. Deprez, C., Lloubès, R., Gavioli, M., Marion, D., Guerlesquin, F., and Blanchard, L. (2005) Solution structure of the *E. coli* TolA C-terminal domain reveals conformational changes upon binding to the phage g3p N-terminal domain. *J. Mol. Biol.* **346,** 1047–1057
13. Bennett, N. J., and Rakonjac, J. (2006) Unlocking of the filamentous bacteriophage virion during infection is mediated by the C domain of pIII. *J. Mol. Biol.* **356,** 266–273
14. Ng, D., Harn, T., Altindal, T., Kolappan, S., Marles, J. M., Lala, R., Spielman, I., Gao, Y., Hauke, C. A., Kovacikova, G., Verjee, Z., Taylor, R. K., Biais, N., and Craig, L. (2016) The *Vibrio cholerae* minor Pilin TcpB initiates assembly and retraction of the toxin-coregulated pilus. *PLoS Pathog.* **12,** e1006109
15. Ford, C. G., Kolappan, S., Phan, H. T., Waldor, M. K., Winther-Larsen, H. C., and Craig, L. (2012) Crystal structures of a CTX pIII domain unbound and in complex with a *Vibrio cholerae* TolA domain reveal novel interaction interfaces. *J. Biol. Chem.* **287,** 36258–36272
16. Lloubès, R., Cascales, E., Walburger, A., Bouveret, E., Lazdunski, C., Bernadac, A., and Journet, L. (2001) The Tol-Pal proteins of the *Escherichia coli* cell envelope: an energized system required for outer membrane integrity? *Res. Microbiol.* **152,** 523–529
17. Sturgis, J. N. (2001) Organisation and evolution of the tol-pal gene cluster. *J. Mol. Microbiol. Biotechnol.* **3,** 113–122
18. Gray, A. N., Egan, A. J., Van't Veer, I. L., Verheul, J., Colavin, A., Koumoutsi, A., Biboy, J., Altelaar, A. M., Damen, M. J., Huang, K. C., Simorre, J. P., Breukink, E., den Blaauwen, T., Typas, A., Gross, C. A., Vollmer, W. (2015) Coordination of peptidoglycan synthesis and outer membrane constriction during *Escherichia coli* cell division. *Elife* **4,** e07118
19. Gully, D., and Bouveret, E. (2006) A protein network for phospholipid synthesis uncovered by a variant of the tandem affinity purification method in *Escherichia coli*. *Proteomics* **6,** 282–293
20. Cascales, E., Gavioli, M., Sturgis, J. N., and Lloubès, R. (2000) Proton motive force drives the interaction of the inner membrane TolA and outer membrane pal proteins in *Escherichia coli*. *Mol. Microbiol.* **38,** 904–915
21. Cascales, E., Lloubès, R., and Sturgis, J. N. (2001) The TolQ–TolR proteins energize TolA and share homologies with the flagellar motor proteins MotA–MotB. *Mol. Microbiol.* **42,** 795–807
22. Walburger, A., Lazdunski, C., and Corda, Y. (2002) The Tol/Pal system function requires an interaction between the C-terminal domain of TolA and the N-terminal domain of TolB. *Mol. Microbiol.* **44,** 695–708
23. Cascales, E., and Lloubès, R. (2004) Deletion analyses of the peptidoglycan-associated lipoprotein Pal reveals three independent binding sequences including a TolA box: Pal interacts independently with OmpA, TolA and TolB. *Mol. Microbiol.* **51,** 873–885
24. Waterhouse, A. M., Procter, J. B., Martin, D. M., Clamp, M., and Barton, G. J. (2009) Jalview Version 2–a multiple sequence alignment editor and analysis workbench. *Bioinformatics* **25,** 1189–1191
25. Gerding, M. A., Ogata, Y., Pecora, N. D., Niki, H., and de Boer, P. A. (2007) The *trans*-envelope Tol-Pal complex is part of the cell division machinery

and required for proper outer-membrane invagination during cell constriction in *E. coli*. *Mol. Microbiol.* **63,** 1008–1025
26. Yeh, Y.-C., Comolli, L. R., Downing, K. H., Shapiro, L., and McAdams, H. H. (2010) The caulobacter Tol-Pal complex is essential for outer membrane integrity and the positioning of a polar localization factor. *J. Bacteriol.* **192,** 4847–4858
27. Santos, T. M., Lin, T.-Y., Rajendran, M., Anderson, S. M., and Weibel, D. B. (2014) Polar localization of *Escherichia coli* chemoreceptors requires an intact Tol-Pal complex: chemoreceptor localization in *Escherichia coli*. *Mol. Microbiol.* **92,** 985–1004
28. Li, C., Zhang, Y., Vankemmelbeke, M., Hecht, O., Aleanizy, F. S., Macdonald, C., Moore, G. R., James, R., and Penfold, C. N. (2012) Structural evidence that colicin A protein binds to a novel binding site of TolA protein in *Escherichia coli* periplasm. *J. Biol. Chem.* **287,** 19048–19057
29. Karimova, G., Pidoux, J., Ullmann, A., and Ladant, D. (1998) A bacterial two-hybrid system based on a reconstituted signal transduction pathway. *Proc. Natl. Acad. Sci. U.S.A.* **95,** 5752–5756
30. Derouiche, R., Zeder-Lutz, G., Bénédetti, H., Gavioli, M., Rigal, A., Lazdunski, C., and Lloubès, R. (1997) Binding of colicins A and El to purified TolA domains. *Microbiology* **143,** 3185–3192
31. Lobstein, J., Emrich, C. A., Jeans, C., Faulkner, M., Riggs, P., and Berkmen, M. (2012) SHuffle, a novel *Escherichia coli* protein expression strain capable of correctly folding disulfide bonded proteins in its cytoplasm. *Microb. Cell Fact.* **11,** 56
32. Martin, A., and Schmid, F. X. (2003) The folding mechanism of a two-domain protein: folding kinetics and domain docking of the gene-3 protein of phage fd. *J. Mol. Biol.* **329,** 599–610
33. Ghrayeb, J., Kimura, H., Takahara, M., Hsiung, H., Masui, Y., and Inouye, M. (1984) Secretion cloning vectors in *Escherichia coli*. *EMBO J.* **3,** 2437–2442
34. Bouveret, E., Rigal, A., Lazdunski, C., and Bénédetti, H. (1998) Distinct regions of the colicin A translocation domain are involved in the interaction with TolA and TolB proteins upon import into *Escherichia coli*. *Mol. Microbiol.* **27,** 143–157
35. Meury, J., and Devilliers, G. (1999) Impairment of cell division in tolA mutants of *Escherichia coli* at low and high medium osmolarities. *Biol. Cell* **91,** 67–75
36. Levengood, S. K., Beyer, W. F., Jr., and Webster, R. E. (1991) TolA: a membrane protein involved in colicin uptake contains an extended helical region. *Proc. Natl. Acad. Sci. U.S.A.* **88,** 5939–5943
37. Buchan, D. W., Minneci, F., Nugent, T. C., Bryson, K., and Jones, D. T. (2013) Scalable web services for the PSIPRED protein analysis workbench. *Nucleic Acids Res.* **41,** W349–W357
38. Tomasi, M., Battistini, A., Araco, A., Roda, L. G., and D'Agnolo, G. (1979) The role of the reactive disulfide bond in the interaction of cholera-toxin functional regions. *Eur. J. Biochem.* **93,** 621–627
39. Craig, L., Pique, M. E., and Tainer, J. A. (2004) Type IV pilus structure and bacterial pathogenicity. *Nat. Rev. Microbiol.* **2,** 363–378
40. Gao, Y., Hauke, C. A., Marles, J. M., and Taylor, R. K. (2016) Effects of tcpB mutations on biogenesis and function of the toxin-coregulated pilus, the type IVb Pilus of *Vibrio cholerae*. *J. Bacteriol.* **198,** 2818–2828
41. Yang, M., Liu, Z., Hughes, C., Stern, A. M., Wang, H., Zhong, Z., Kan, B., Fenical, W., and Zhu, J. (2013) Bile salt-induced intermolecular disulfide bond formation activates *Vibrio cholerae* virulence. *Proc. Natl. Acad. Sci. U.S.A.* **110,** 2348–2353
42. Morgan, S. J., French, E. L., Thomson, J. J., Seaborn, C. P., Shively, C. A., and Krukonis, E. S. (2015) Formation of an intramolecular periplasmic disulfide bond in TcpP protects TcpP and TcpH from degradation in *Vibrio cholerae*. *J. Bacteriol.* **198,** 498–509
43. Fengler, V. H., Boritsch, E. C., Tutz, S., Seper, A., Ebner, H., Roier, S., Schild, S., and Reidl, J. (2012) Disulfide bond formation and ToxR activity in *Vibrio cholerae*. *PLoS ONE* **7,** e47756
44. Battesti, A., and Bouveret, E. (2012) The bacterial two-hybrid system based on adenylate cyclase reconstitution in *Escherichia coli*. *Methods* **58,** 325–334
45. Ouellette, S. P., Gauliard, E., Antosová, Z., and Ladant, D. (2014) A Gateway®-compatible bacterial adenylate cyclase-based two-hybrid system. *Environ. Microbiol. Rep.* **6,** 259–267
46. Handford, J. I., Ize, B., Buchanan, G., Butland, G. P., Greenblatt, J., Emili, A., and Palmer, T. (2009) Conserved network of proteins essential for bacterial viability. *J. Bacteriol.* **191,** 4732–4749
47. Houot, L., Fanni, A., de Bentzmann, S., and Bordi, C. (2012) A bacterial two-hybrid genome fragment library for deciphering regulatory networks of the opportunistic pathogen *Pseudomonas aeruginosa*. *Microbiology* **158,** 1964–1971
48. Gaspar, J. A., Thomas, J. A., Marolda, C. L., and Valvano, M. A. (2000) Surface expression of O-specific lipopolysaccharide in *Escherichia coli* requires the function of the TolA protein. *Mol. Microbiol.* **38,** 262–275
49. Dennis, J. J., Lafontaine, E. R., and Sokol, P. A. (1996) Identification and characterization of the tolQRA genes of *Pseudomonas aeruginosa*. *J. Bacteriol.* **178,** 7059–7068
50. Lorenz, S. H., Jakob, R. P., Weininger, U., Balbach, J., Dobbek, H., and Schmid, F. X. (2011) The filamentous phages fd and IF1 use different mechanisms to infect *Escherichia coli*. *J. Mol. Biol.* **405,** 989–1003
51. Basse, M. J., Betzi, S., Bourgeas, R., Bouzidi, S., Chetrit, B., Hamon, V., Morelli, X., and Roche, P. (2013) 2P2Idb: a structural database dedicated to orthosteric modulation of protein/protein interactions. *Nucleic Acids Res.* **41,** D824–D827
52. Basse, M.-J., Betzi, S., Morelli, X., and Roche, P. (2016) 2P2Idb v2: update of a structural database dedicated to orthosteric modulation of protein/protein interactions. *Database* 2016 baw007
53. Bonsor, D. A., Hecht, O., Vankemmelbeke, M., Sharma, A., Krachler, A. M., Housden, N. G., Lilly, K. J., James, R., Moore, G. R., and Kleanthous, C. (2009) Allosteric β-propeller signalling in TolB and its manipulation by translocating colicins. *EMBO J.* **28,** 2846–2857
54. Sinha, N., and Smith-Gill, S. J. (2002) Electrostatics in protein binding and function. *Curr. Protein Pept. Sci.* **3,** 601–614
55. Faruque, S. M., Asadulghani, Saha, M. N., Alim, A. R., Albert, M. J., Islam, K. M., and Mekalanos, J. J. (1998) Analysis of clinical and environmental strains of nontoxigenic *Vibrio cholerae* for susceptibility to CTXΦ: molecular basis for origination of new strains with epidemic potential. *Infect. Immun.* **66,** 5819–5825
56. Hasan, N. A., Ceccarelli, D., Grim, C. J., Taviani, E., Choi, J., Sadique, A., Alam, M., Siddique, A. K., Sack, R. B., Huq, A., and Colwell, R. R. (2013) Distribution of virulence genes in clinical and environmental *Vibrio cholerae* strains in Bangladesh. *Appl. Environ. Microbiol.* **79,** 5782–5785
57. Ceccarelli, D., Chen, A., Hasan, N. A., Rashed, S. M., Huq, A., and Colwell, R. R. (2015) Non-O1/non-O139 *Vibrio cholerae* carrying multiple virulence factors and *V. cholerae* O1 in the Chesapeake Bay, Maryland. *Appl. Environ. Microbiol.* **81,** 1909–1918
58. Jiang, S., Chu, W., and Fu, W. (2003) Prevalence of cholera toxin genes (ctxA and zot) among non-O1/O139 *Vibrio cholerae* strains from Newport Bay, California. *Appl. Environ. Microbiol.* **69,** 7541–7544
59. Sarkar, A., Nandy, R. K., Nair, G. B., and Ghose, A. C. (2002) *Vibrio* pathogenicity island and cholera toxin genetic element-associated virulence genes and their expression in non-O1 non-O139 strains of *Vibrio cholerae*. *Infect. Immun.* **70,** 4735–4742
60. Boyd, E. F., Moyer, K. E., Shi, L., and Waldor, M. K. (2000) Infectious CTXΦ and the *Vibrio* pathogenicity island prophage in *Vibrio* mimicus: evidence for recent horizontal transfer between *V. mimicus* and *V. cholerae*. *Infect. Immun.* **68,** 1507–1513
61. Bille, E., Zahar, J.-R., Perrin, A., Morelle, S., Kriz, P., Jolley, K. A., Maiden, M. C., Dervin, C., Nassif, X., and Tinsley, C. R. (2005) A chromosomally integrated bacteriophage in invasive meningococci. *J. Exp. Med.* **201,** 1905–1913
62. Derbise, A., Chenal-Francisque, V., Pouillot, F., Fayolle, C., Prévost, M.-C., Médigue, C., Hinnebusch, B. J., and Carniel, E. (2007) A horizontally acquired filamentous phage contributes to the pathogenicity of the plague *Bacillus*. *Mol. Microbiol.* **63,** 1145–1157
63. Gonzalez, M. D., Lichtensteiger, C. A., Caughlan, R., and Vimr, E. R. (2002) Conserved filamentous prophage in *Escherichia coli* O18:K1:H7 and *Yersinia pestis* biovar *orientalis*. *J. Bacteriol.* **184,** 6050–6055
64. Goforth, J. B., Walter, N. E., and Karatan, E. (2013) Effects of polyamines on *Vibrio cholerae* virulence properties. *PLoS ONE* **8,** e60765
65. Metcalf, W. W., Jiang, W., Daniels, L. L., Kim, S. K., Haldimann, A., and Wanner, B. L. (1996) Conditionally replicative and conjugative plasmids

carrying lacZ α for cloning, mutagenesis, and allele replacement in bacteria. *Plasmid* **35,** 1–13
66. Houot, L., and Watnick, P. I. (2008) A novel role for enzyme I of the *Vibrio cholerae* phosphoenolpyruvate phosphotransferase system in regulation of growth in a Biofilm. *J. Bacteriol.* **190,** 311–320
67. Li, M. Z., and Elledge, S. J. (2007) Harnessing homologous recombination in vitro to generate recombinant DNA via SLIC. *Nat. Methods* **4,** 251–256
68. Jeong, J.-Y., Yim, H.-S., Ryu, J.-Y., Lee, H. S., Lee, J.-H., Seen, D.-S., and Kang, S. G. (2012) One-step sequence- and ligation-independent cloning as a rapid and versatile cloning method for functional genomics studies. *Appl. Environ. Microbiol.* **78,** 5440–5443
69. van den Ent, F., and Löwe, J. (2006) RF cloning: a restriction-free method for inserting target genes into plasmids. *J. Biochem. Biophys. Methods.* **67,** 67–74
70. Guzman, L.-M., Belin, D., Carson, M. J., and Beckwith, J. O. (1995) Tight regulation, modulation, and high-level expression by vectors containing the arabinose PBAD promoter. *J. Bacteriol.* **177,** 4121–4130
71. Das, B., Bischerour, J., Val, M.-E., and Barre, F.-X. (2010) Molecular keys of the tropism of integration of the cholera toxin phage. *Proc. Natl. Acad. Sci. U.S.A.* **107,** 4377–4382
72. Kirn, T. J., Lafferty, M. J., Sandoe, C. M., and Taylor, R. K. (2000) Delineation of pilin domains required for bacterial association into microcolonies and intestinal colonization by *Vibrio cholerae*. *Mol. Microbiol.* **35,** 896–910
73. McWilliam, H., Li, W., Uludag, M., Squizzato, S., Park, Y. M., Buso, N., Cowley, A. P., and Lopez, R. (2013) Analysis Tool Web Services from the EMBL-EBI. *Nucleic Acids Res.* **41,** W597–W600